PHYSICAL REVIEW B **74**, 100404(R) (2006)

Interaction of magnetostatic excitations with 90° domain walls in micrometer-sized permalloy squares

M. Buess,[1] J. Raabe,[1] K. Perzlmaier,[2] C. H. Back,[2] and C. Quitmann[1]
[1]*Paul Scherrer Institut, CH-5232 Villigen PSI, Switzerland*
[2]*Institut für Experimentelle und Angewandte Physik, Universität Regensburg, Universitätsstrasse 31, D-93040 Regensburg, Germany*
(Received 13 June 2006; revised manuscript received 30 August 2006; published 27 September 2006)

We investigate the magnetic excitations in soft magnetic squares and in particular the role of domain walls in such Landau flux-closure structures. For this we combine synchrotron-based photoemission electron microscopy and simulations using the Landau-Lifshitz-Gilbert equation. We show that the 90° Néel walls in such squares act as efficient barriers for magnetic excitations that absorb the incoming energy. Because of the finite elasticity, the absorbed energy leads to oscillations of the domain walls, which subsequently cause emission of sharp wave fronts.

DOI: 10.1103/PhysRevB.74.100404 PACS number(s): 75.40.Gb, 75.75.+a, 75.30.Ds

Magnetization dynamics is a field that has received considerable attention in recent years. Besides its fundamental interest, magnetization dynamics in the precessional regime—typically on the picosecond time scale—has also found its way into potential device applications. These range from precessional switching schemes in magnetic random access memory cells to a revived interest in microwave devices made of magnetic materials such as microwave isolators, circulators, resonators, filters, or phase shifters.[1–5] Magnetic thin-film devices possess certain peculiarities that make them interesting for device applications. First of all, the frequency of the precessing magnetization may be tuned by external magnetic fields; second, thin-film structures can be made compact in size; third, thin magnetic films show interesting spin wave dispersions with branches of positive and negative dispersion. One possible device that one can imagine is a spin wave phase shifter. Recently, Hertel *et al.* have shown—using micromagnetic simulations—that 180° or 360° Néel domain walls placed in a narrow permalloy ($Ni_{81}Fe_{19}$) strip act as a phase shifter for traveling spin wave excitations.[6] In both cases, the domain walls are obviously transparent for magnetic excitations. Less is known about the effect of 90° Néel walls on magnetic excitations. In recent publications it has been shown that time-resolved x-ray photoemission electron microscopy (XPEEM) is a sensitive tool that can be used to study the temporal response of magnetic micro- and nanostructures with high temporal and spatial resolution.[7–10]

In this Rapid Communication we focus on the influence of 90° Néel domain walls on magnetic excitations in permalloy squares with a side length of 5 μm which are in the flux-closure domain configuration. We use time-resolved XPEEM in two different geometries that allow us to analyze the magnetization dynamics in all four domains under equivalent excitation geometries and with equal sensitivity. Our results and comparison to micromagnetic simulations indicate that 90° Néel domain walls are not transparent to magnetostaticlike excitations. However, excitations are generated at the moving domain walls, which subsequently radiate out into the large domains.

The torque $\boldsymbol{T} \propto \boldsymbol{M} \times \boldsymbol{H}_{\mathrm{p}}$ exerted on the local magnetization by a tipping field pulse $\boldsymbol{H}_{\mathrm{p}}$ is the driving force for the magnetic excitations. The strength and sign of the initial torque are determined by the strength and direction of $\boldsymbol{H}_{\mathrm{p}}$ and the orientation of the local magnetization in the sample. The initial torque determines how a magnetic system is excited. Subsequently, the micromagnetic structure determines how the energy deposited into the system is converted into magnetic excitations. In the following we will distinguish three types of magnetic excitations. (i) Magnetostatic spin waves are long-wavelength excitations that are dominated by the dipolar interaction.[11–14] (ii) The domain wall mode is exchange dominated and located in the domain walls. (iii) The vortex gyrotropic mode[7,15,16] describes the motion of the vortex core. We study permalloy squares of 5 μm side length and 20 nm thickness placed on top of a coplanar waveguide (gold, 10 μm width, 200 nm thickness). The samples are imaged using time-resolved XPEEM at the Surface/Interface: Microscopy beamline of the Swiss Light Source (SLS).[17] PEEM records the x-ray absorption coefficient with a spatial resolution of $\approx$100 nm. Pure x-ray magnetic circular dichroic (XMCD) contrast is obtained by taking two images at the Fe L_3 absorption edge differing only in the circular polarization ($+\boldsymbol{P}$ and $-\boldsymbol{P}$). Taking their ratio eliminates all topographic and chemical contrast.[18] The intensity is then proportional to the scalar product $\boldsymbol{M}(\boldsymbol{r}) \cdot \boldsymbol{P}$. Time-resolved experiments are performed using a stroboscopic pump-probe technique. A pulsed laser ($t_{FWHM} \approx 12$ ps) illuminates a photodiode launching a current pulse into a coplanar wave guide. This creates a magnetic field pulse exciting the magnetization. The sample is probed using an x-ray pulse produced by an isolated electron bunch ($t_{FWHM} \approx 80$ ps) located in a 180 ns gap of the filling pattern of the SLS storage ring. All other x-ray pulses are suppressed by gating the detector. Pump and probe pulses are synchronized with a variable electronic delay Δt. The sample is excited every 16 ns and is probed every 1.04 μs. To acquire an image we typically integrate the signal for 200 s, thus averaging over 2×10^8 pump-probe cycles.

Our experimental technique based on the XMCD contrast is sensitive to the intensity $I = \boldsymbol{M}(\boldsymbol{x},t) \cdot \boldsymbol{P}$, where $\boldsymbol{P}$ is the photon propagation direction and $\boldsymbol{M}(\boldsymbol{x},t)$ is the sum of the static and dynamic parts of the magnetization $\boldsymbol{M}(\boldsymbol{x},t) = \boldsymbol{M} + \boldsymbol{m}(t)$. Therefore, domains with magnetization direction collinear to

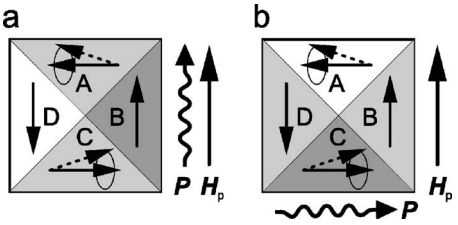

FIG. 1. Two geometries to probe the magnetization dynamics of the sample. (a) The photon direction $\boldsymbol{P}$ is parallel to the field pulse direction $\boldsymbol{H}_{\mathrm{p}}$, and static magnetic contrast is visible in domains B and D, indicated by the black and white contrast. (b) In this geometry we are sensitive to the precession of the magnetization in domains B and D while the static contrast appears in domains A and C.

the photon propagation direction give maximum contrast in a *static* experiment. However, the sensitivity to the *dynamic* part $\boldsymbol{m}(t)$ of the magnetization vector is proportional to $\sin(\delta) \propto \delta$ for $\boldsymbol{M} \perp \boldsymbol{P}$ and proportional to $\cos(\delta) \propto 1-\delta^2/2$ for $\boldsymbol{M} \| \boldsymbol{P}$, where δ is the angular change. To observe both the static ($\boldsymbol{M}$) and dynamic [$\boldsymbol{m}(t)$] components of the magnetization in all four domains we have to use the two measurement geometries described in Fig. 1. In Fig. 1(a) we are measuring the y component of $\boldsymbol{m}(t)$ in domains A and C, while in (b) we are measuring the x component of $\boldsymbol{m}(t)$ in domains B and D. We would like to emphasize that in the geometries described above the initial torque is maximal in domains A and C, while it is zero in domains B and D.

In the experiment we now record XMCD image series as a function of time elapsed after the disturbing field pulse $\boldsymbol{H}_{\mathrm{p}}$ (see Ref. 8). The data are also available as online movies.[20] In a first step, high-symmetry points of the time-resolved image series are analyzed. The signal is extracted from the XMCD image series in circular areas of 0.8 μm diameter exactly in the centers of the domains for both magnetization components. The results for two neighboring domains are summarized in Fig. 2. For the geometry of Fig. 2(a) we see a pronounced dynamic magnetization $\boldsymbol{m}_y^{\mathrm{C}}$ in domain C while we observe no sign of precessional motion in the signal $\boldsymbol{m}_y^{\mathrm{B}}$ from domains B [Fig. 2(a)]. When we turn to the geometry of Fig. 2(b) we still pick up a dynamic signal $\boldsymbol{m}_x^{\mathrm{C}}$ in domain C due to the large in-plane deviation of $\boldsymbol{m}^{\mathrm{C}}$ of 22°. For a large-angle elliptical precession[23] we expect to pick up a dynamic magnetization signal also along the x direction. We also note that the signal $\boldsymbol{m}_x^{\mathrm{C}}$ is expected to oscillate at twice the frequency of $\boldsymbol{m}_y^{\mathrm{C}}$ measured in Fig. 2(a), which is not observed. The reasons for this are the following. First, there is a significant effect from the domain wall that modifies the response in the center of the domain. This is already an indication that this cannot be described by a "macrospin" approach. Second, the two components $\boldsymbol{m}_x$ and $\boldsymbol{m}_y$ were measured in two separate runs of the experiment with differing pulse amplitude ($\boldsymbol{H}_{\mathrm{p}}$=30 Oe for $\boldsymbol{m}_x$ and 20 Oe for $\boldsymbol{m}_y$). The shape of the field pulse is provided as auxiliary material.[20]

However, in domains B we still do not pick up any dynamic signal $\boldsymbol{m}_x^{\mathrm{B}}$, even though these are the domains where we have maximum sensitivity to the dynamic magnetization. We conclude from this result that, within our experimental

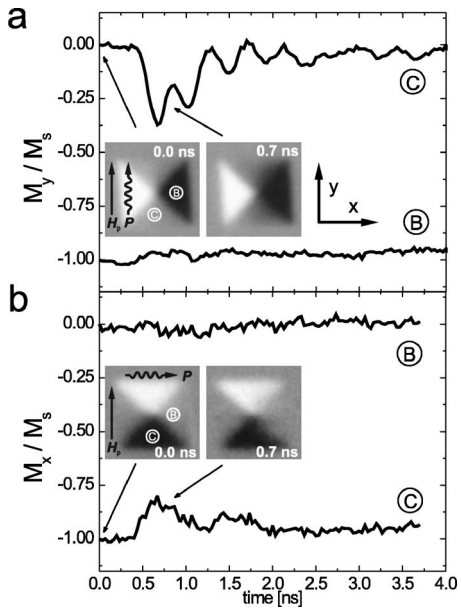

FIG. 2. Magnetic excitations in the domain center for the two geometries. The insets show snapshots of the dichroic images at 0.0 ns (before the external field pulse) and at 0.7 ns (near the peak of the pulse). (a) shows M_y and (b) shows M_x.

accuracy, the precessional motion excited by the initial torque $\boldsymbol{T}$ in the center of the domains A and C is not transmitted through the domain walls, or the signal is averaged out at the location of the analyzed region.

In Fig. 2 we have investigated points of high symmetry. We can refine our findings by analyzing also nonsymmetrical positions. In Fig. 3(b) we show line scans as a function of time extracted from the image series through domain A (left side) and through domain B (right side) as illustrated in Fig. 3(a). The raw data for the y component (x component) of $\boldsymbol{M}$ are shown in Fig. 3(b) left [Fig. 3(b) right], respectively. Notice that the white (black) contrast at the top (bottom) corresponds to the areas where we are sensitive to the static magnetization $\boldsymbol{M}$, while regions in gray correspond to areas where we are sensitive to the dynamic magnetization $\boldsymbol{m}(t)$. Already in the raw data we observe a dynamic signal in Fig. 3(b) for both geometries in contrast to the data shown in Figure 2. To further analyze our findings and to achieve higher sensitivity to the dynamic magnetization, we subtract the first image of the full sequence, which corresponds to the static magnetization before the tipping field pulse arrives [see Fig. 3(c)]. It is now obvious that the precessional response measured in domain A is more or less in phase across the whole domain, while in domain B the response is 180° out of phase when measured at the positions 3 and 4 [see Fig. 3(d)]. In fact, the averaging performed in Fig. 2 eliminates the contrast. It is important to realize that the change of contrast observed in domain B is smaller by a factor of 4 when compared to the one in domain A. Furthermore, the contrast in domain A is largest shortly after the tipping field pulse has excited the magnetization (at about 0.8 ns) and subsequently relaxes back toward its static value. In contrast, the maximum precessional response at about 1.2 ns near the center of domain B is delayed by about 400 ps. We conclude

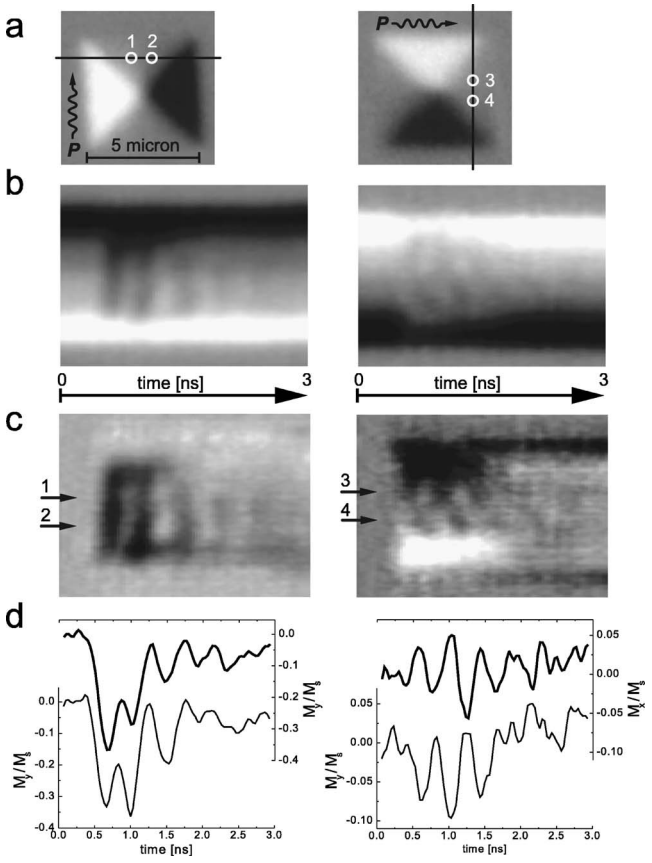

FIG. 3. Line scan across the sample as depicted in (a) in the two geometries (left and right). The resulting data are plotted along the time axis to produce a combined space-time plot (b). To focus on the dynamical part, the first line at $t=0$ is subtracted from the data in the space-time plots (c). In (d), the signal is extracted from (c) at positions 1–4.

that the 90° domain walls are not transparent to the magnetostatic excitation generated in domains A and C in contrast to the response predicted for spin waves traveling through 180° or 360° walls in Ref. 6. This finding has already been observed in micromagnetic simulations where only one domain was excited locally.[19]

The observed response in domains B and D calls for an explanation. Three possibilities arise. (i) The tipping field pulse excites also domains B and D as the magnetization may not be absolutely perpendicular to the field pulse close to the domain wall (DW). (ii) The excitation is generated by the initial torque acting on the magnetization in domains A and C; it traverses the domain wall with a reduced amplitude and travels toward the center of domains B and D, where we pick up the signal. (iii) The magnetic excitation is generated at the moving domain walls.

Scenario (i) can be excluded as we would then expect a similar timing of the response in domains B,D as observed in domains A,C with a maximum excitation shortly after the field pulse has triggered the precessional motion of the magnetization.

Scenarios (ii) and (iii) are difficult to disentangle. In the following we suggest that in fact an excitation seems to be generated at the moving domain walls, but is driven by the

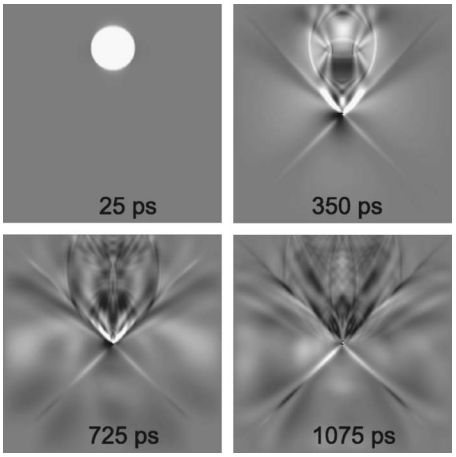

FIG. 4. Micromagnetic simulation with inhomogeneous excitation showing snapshots of $\boldsymbol{M}_z(t)-\boldsymbol{M}_z(t=0)$. Upper row: Spin waves emanate at the bright region and spread in the upper domain. Lower row: The wave front reaches the DW but does not cross it; its energy is partly reflected and partly absorbed, leading to an excitation localized in the DW. This sends out new wave fronts into the neighboring domains.

excitation within domains A and C. In Ref. 8 we have shown that, as a consequence of the strong tipping field pulse in the plane of the element, the vortex is moving perpendicular to the direction of the field pulse. The vortex core is displaced along the negative x direction after the field pulse. In addition, the domain walls bend. This can be seen in the snapshots at 0.7 ns of Fig. 2: On one side of the square, domain B gets enlarged because the domain walls are bending into domains A and C while on the other side of the square domain D decreases in size. This results in a difference of the dynamics in the two domains. In fact, if we analyze the data in the frequency domain over the accessible period of 3 ns, we notice that the precessional frequencies in domain B and D differ significantly (the main peaks are at 2.2 GHz in domain B and 2.5 GHz in domain D). The asymmetries in the two domains have also been observed in larger permalloy squares.[21,22] They observe the formation of spike domains.

To better understand our experimental findings, we have performed micromagnetic simulations.[24] In a first step we have used the temporal and spatial pulse shape extracted from the data for modeling the simulation. The results (not shown) are in good agreement with the data. However, if we address the question of domain wall transparency, scenarios (ii) and (iii) still cannot be disentangled. In a second approach, a 5 Oe strong and 50 ps long rectangular field pulse is applied to a circular area in the center of domain A. In the first image of Fig. 4 this region can be clearly seen. With this configuration we can be sure that the other regions, namely, the neighboring domains and the domain walls, are not directly excited by the field pulse. The simulation leads to the following results. Initially the field pulse creates an excitation and spin waves propagate toward the domain walls. However, these spin waves are not transmitted through the DW but mostly reflected back into domain A. In addition, the reflection process stimulates the domain wall itself, which starts to oscillate. At this stage the excited DW is able to

radiate spin waves into the neighboring domains as well. The spin waves that are radiated off the domain walls show a different shape than the ones initially excited by the magnetic field pulse: the circular geometry is lost and the wave fronts roughly have the linear shape of the domain walls (see image at 725 ps in Fig. 4). Thus the oscillations in domains B and D are not spin waves propagated from domain A, but spin waves emitted from the DW, which in turn has been excited by the dynamics in domain A. The data are also available as an online movie.[20]

In summary, we have investigated the spin dynamics in Landau structures and especially the effect of 90° Néel walls on magnetic excitations. We have presented experimental data using time-resolved PEEM microscopy where both in-plane components of $\boldsymbol{M}$ have been measured, and micromagnetic simulations using the Landau-Lifshitz-Gilbert code. The external field pulse initially excites two domains (A and C) and the domain walls directly. From our data we conclude that the domain wall is an effective barrier for the excitation of nearby domains. However, the wall is not a passive object but is active and responsible for the antisymmetric excitations in domains B and D. The excitation is generated near the domain wall, and propagates with a speed of 1.3 μm/ns toward the domain center. This agrees with the observed delay of the excitation in Fig. 3(d) (right). Furthermore, the domain wall is able to emit spin waves with sharp wave fronts.

We gratefully acknowledge D. Weiss for clean room access.

[1] R. P. Cowburn and M. E. Welland, Science **287**, 1466 (2000).
[2] Y. K. Fetisov and C. E. Patton, IEEE Trans. Magn. **35**, 1024 (1999).
[3] A. B. Ustinov and B. A. Kalinikov, Tech. Phys. Lett. **27**, 403 (2001).
[4] M. P. Kostylev, A. A. Serga, T. Schneider, B. Leven, and B. Hillebrands, Appl. Phys. Lett. **87**, 153501 (2005).
[5] K. Potzger, L. Bischoff, M. O. Liedke, B. Hillebrands, M. Rickart, P. P. Freitas, J. McCord, and J. Fassbender, IEEE Trans. Magn. **41**, 3610 (2005).
[6] R. Hertel, W. Wulfhekel, and J. Kirschner, Phys. Rev. Lett. **93**, 257202 (2004).
[7] S.-B. Choe, Y. Acremann, A. Scholl, A. Bauer, A. Doran, J. Stöhr, and H. A. Padmore, Science **304**, 420 (2004).
[8] J. Raabe, C. Quitmann, C. H. Back, F. Nolting, S. Johnson, and C. Buehler, Phys. Rev. Lett. **94**, 217204 (2005).
[9] A. Krasyuk, F. Wegelin, S. A. Nepijko, H. J. Elmers, G. Schönhense, M. Bolte, and C. M. Schneider, Phys. Rev. Lett. **95**, 207201 (2005).
[10] K. Yu. Guslienko, X. F. Han, D. J. Keavney, R. Divan, and S. D. Bader, Phys. Rev. Lett. **96**, 067205 (2006).
[11] Y. Acremann, C. H. Back, M. Buess, O. Portmann, A. Vaterlaus, D. Pescia, and H. Melchior, Science **290**, 492 (2000).
[12] J. P. Park, P. Eames, D. M. Engebretson, J. Berezovsky, and P. A. Crowell, Phys. Rev. B **67**, 020403(R) (2003).
[13] M. Buess, R. Höllinger, T. Haug, K. Perzlmaier, U. Krey, D. Pescia, M. R. Scheinfein, D. Weiss, and C. H. Back, Phys. Rev. Lett. **93**, 077207 (2004).
[14] K. Perzlmaier, M. Buess, C. H. Back, V. E. Demidov, B. Hillebrands, and S. O. Demokritov, Phys. Rev. Lett. **94**, 057202 (2005).
[15] B. E. Argyle, E. Terrenzio, and J. C. Slonczewski, Phys. Rev. Lett. **53**, 190 (1984).
[16] H. Stoll, A. Puzic, B. van Waeyenberge, P. Fischer, J. Raabe, M. Buess, T. Haug, R. Höllinger, C. H. Back, D. Weiss, and G. Denbeaux, Appl. Phys. Lett. **84**, 3328 (2004).
[17] C. Quitmann, U. Flechsig, L. Patthey, T. Schmidt, G. Ingold, M. Howells, M. Janousch, and R. Abela, Surf. Sci. **480**, 173 (2001).
[18] G. Schoenhense, J. Phys.: Condens. Matter **11**, 9517 (1999).
[19] M. Münzenberg *et al.* (unpublished).
[20] See EPAPS Document No. E-PRBMDO-74-R08634 for movies. This document can be reached via a direct link in the online article's HTML reference section or via the EPAPS homepage (http://www.aip.org/pubservs/epaps.html).
[21] C. M. Schneider, A. Kuksov, A. Krasyuk, A. Oelsner, D. Neeb, S. A. Nepijko, G. Schönhense, I. Mönch, R. Kaltofen, J. Morais, C. de Nadaï, and N. B. Brookes, Appl. Phys. Lett. **85**, 2562 (2004).
[22] A. Neudert, J. McCord, D. Chumakov, R. Schäfer, and L. Schultz, Phys. Rev. B **71**, 134405 (2005).
[23] We do not expect a signal from the out-of-plane component z. With a grazing angle of 16° of the photon propagation direction with respect to the sample plane, a deviation of $\boldsymbol{M}$ along the z direction contributes with a factor of 0.287 (compared to the in-plane component) to the magnetic contrast. Due to the demagnetizing field an elliptical precessional motion with an aspect ratio of the z component to the in-plane component of 1:10 is expected, which further suppresses the signal expected from the z component to below 3%.
[24] Micromagnetic simulations using the LLG code have been performed for comparison and detailed analysis of the experiment. In our simulations we use the following parameters. The sample thickness, cell size, saturation magnetization, exchange stiffness, gyromagnetic ratio, and damping constant are 20 nm, $5\times5\times20$ nm^3, 860 kA/m, 13×10^{-12} J/m, 176 GHz/T, and 0.008, respectively. As a tipping field pulse we use the experimentally observed one (Ref. 20). Information on the LLG code can be found at http://llgmicro.home.mindspring.com/